I S A V

Journal of Theoretical and Applied

Vibration and Acoustics

journal homepage: http://tava.isav.ir

In-plane and out–of-plane free vibration in nano ultra-thin film using a general nonlocal Kirchhoff ultra-thin film model

Arash Rahmani[a], **Ahad Ahmadpour fard**[b], **Shirko Farooghi**[a*]

[a] *Professor, Urmia University of Technology, Urmia, Iran*

[b] *MSc Student, Urmia University of Technology, Urmia, Iran*

ARTICLE INFO

Article history:
Received 8 October 2019

Received in revised form
5 February 2020

Accepted 19 June 2020

Available online 28 June 2020

Keywords:
Free vibration,

Kirchhoff nano ultra-thin film,

Differential Quadrature Method,
General nonlocal theory.

ABSTRACT

In this paper, the in-plane and out-plane free vibration of the Kirchhoff nano ultra-thin film are studied. To reveal the altering natures of natural frequencies in nano ultra-thin film, the film is modeled according to the general nonlocal theory (GNT). The film governing equations as well as the characteristics eigenvalues equations are established depending on two different nonlocal parameters. The existence of these different nonlocal parameters causes the model to be able to predict both increase and reduction of stiffness in nano ultra-thin film. Here, the differential quadrature method (DQM) is applied for obtaining the natural frequencies of in-plane and out of plane. An intensive parametric study is carried out on the natural frequencies of nano ultra-thin film. The results reveal that the effect of nonlocal parameters on the frequency parameter is more prominent at the higher aspect ratios.

© *2020 Iranian Society of Acoustics and Vibration, All rights reserved.*

1. Introduction

In recent years, the applications of micro/nano structures have been growing because of their outstanding electrical, thermal, and mechanical properties. Accordingly, the accurate evaluation and detailed study of the mechanical behaviors of micro/nano structures are necessary to increase their reliability and obtain the proper design of small-scaled systems. In recent years, due to the shortcoming of the classical continuum mechanics theories in analyzing the mechanical behaviors of small-scaled (micro/nano) structures, non-classical elasticity theories such as Eringen's nonlocal theory (ENT), modified couple-stress theory (MCST), strain gradient theory (SGT) and etc. are developed and considered extensively [1-8]. Many researchers have

* Corresponding author:
E-mail address: sh.farughi@uut.ac.ir(Sh.Farooghi)

http://dx.doi.org/10.22064/tava.2021.115465.1148

considered the mechanical behaviors of micro/nano structures in recent years [9-16]. The following literature review is allocated to the investigation of the mechanical vibrational behaviors of such small-scaled elements.

Sourki and Hosseini [17] proposed the analysis of the vibrational behavior of a nanobeam with consideration of surface effects. They employed Euler-Bernoulli beam model with ENT and MSCT in their contribution. Khaniki [18] considered combined local and nonlocal Eringen's elasticity to analyze the vibrational behavior of rotating Euler-Bernoulli nanobeam. Arvin [19] considered the free vibrational behavior of microbeams based on MCST and TBT via differential transform method. Ansari et al.[20] .used the surface stress elasticity theory to study the nonlinear forced vibration of nanobeam. They applied GDQM and Galerkin-based numerical approaches to make the results. Khaniki [21] presented the vibration analysis of FG Euler-Bernoulli nanobeams employing two-phase Eringen's model. Bhattacharya and Das [22] presented a free vibration analysis of a 2D-FG rotating micro-beam. They employed MSCT and Timoshenko beam theory to derived their model. Pradhan and Murmu [23] considered bending and vibration of rotating nano-cantilever using nonlocal Eringen's model. Fang et al. [24, 25] established a 3D model of rotating FG Euler–Bernoulli microbeam considering MCST. They utilized Ritz method and second-kind Lagrange's formulation and studied the axial, chord-wise, and flap-wise motions. Talebitooti et al. [26] expressed the vibrational behavior of a rotating FG nanobeam. They employed Eringen's model and differential transformation method (DFM) to establish the.

Mirjavadi et al.[27] employed MCST and TBT to study the effect of temperature and porosity on vibrational behavior of 2D- FG microbeams. Roque et al.[28] studied the effect of small-scale factors on the vibration of Timoshenko FG nanobeam. Shafiei et al. [29] expressed vibration analysis of 2D-FG nanobeam using both Eringen's and couple stress theories separately. They studied two different kinds of porous materials and also various BCs.

Shahidi et al.[30] studied vibration characteristics of nonuniform orthotropic nano-scaled plates. They employed ENT to extract the model and used FEM to solve and find the results. Arefi et al. [31] presented vibration analysis of 3-layered nano-plate with graphene core and piezo-magnetic face sheets embedded on Pasternak's foundation. They applied Eringen's nonlocal theory and FSDT to establish equations of motion and used Navier method to solve the problem. Ebrahimi and Barati [32] developed vibrational analyses of a nano-plate resting on a viscoelastic foundation. They considered nonlocal strain gradient theory and Kelvin–Voit model in their studies. They implemented Galerkin numerical method to find the results. Karimi et al.[33] employed nonlocal strain gradient model with SSDT to study free vibration of FG nano-plates resting on Kerr foundation. Liu *et al*. [34] investigated vibration analysis of piezomagnetic nano-plate with laminated composite core. nonlocal strain gradient and Mindlin plate theories are considered to make the model. Daikh et al. [35] illustrated the vibrational behavior of FG nano-plate with thermal effect. Eringen's nonlocal and Navier's solution are applied in the study. Faroughi and Goushegir [36] considered free in-plane vibration of non-uniform nano-plate using Eringen's nonlocal theory and Ritz method. Rahaimi et al.[37] studied in-plane Eringen's nonlocal vibration of FG nano-plate considering thermoelastic damping.

Among the non-classical elasticity theories, general nonlocal theory (GNT) is the most reliable one because of its abilities to capture both hardening and softening behaviors of the material [38-40] and according to the above literature review, it was found that the existing investigations on

vibration (in-plane and out-plane) analysis in small-scaled nano-plates are mainly based on the Eringen's, strain gradient, modified couple stress, and especially nonlocal strain gradient theories; and general nonlocal theory has not been considered until now. Hence,in the present paper, the general nonlocal theory is employed to express the vibrational behavior of Kirchhoff ultra-thin film. To this, general nonlocal theory and Hamilton's principle are considered to derive the governing equations of in-plane and out-plane motions. Then, DQM is employed to solve the problem and extract the numerical results. In the current study, in addition to this novel consideration, the current comprehensive study encompasses the interactions of two nonlocal length scale parameters, aspect ratio, boundary conditions, and mode number on the Kirchhoff nano ultra-thin film.

2. Governing equations

2.1. The general nonlocal theory

Based on the general nonlocal theory, which is developed by Shaat and Abdelkefi [38], the material is expressed by 2 different nonlocal parameters to consider the normal and shear strains fields. The general nonlocal theory outweighs Eringen's nonlocal theory in utilizing different nonlocal parameters for the different coefficients. According to the general nonlocal theory, the differential form of the constitutive model is expressible as the following [38]:

$$(1-\varepsilon_1\nabla^2)(1-\varepsilon_2\nabla^2)t_{(ji)}(x)=\lambda(1-\varepsilon_2\nabla^2)\varepsilon_{rr}\delta_{ij}+2\mu(1-\varepsilon_1\nabla^2)\varepsilon_{ij} \tag{1}$$

In which, $t_{(ji)}$ is a symmetric nonlocal stress tensor. $\nabla^2=(\frac{\partial^2}{\partial x^2}+\frac{\partial^2}{\partial y^2}+\frac{\partial^2}{\partial z^2})$ is Laplacian operator. ε_1 and ε_2 are two constant nonlocal parameters which depend on the selected material. λ and μ Lame's parameters and defined as $\mu=\frac{E}{2(1+\nu)}$, $\lambda=\frac{E\nu}{(1+\nu)(1-2\nu)}$. E is the modulus of elasticity and μ is the shear modulus.

It should be mentioned that Eringen's nonlocal theory is recovered if $\varepsilon_1=\varepsilon_2$ [38].

2.2. Equations of motion

Here, we investigate the vibration of ultra-thin film based on the general nonlocal theory [26]. Kirchhoff Plate's assumptions are considered to model the displacement field of the thin film:

$$\begin{aligned} u(x,y,z)&=u_0(x,y,t)-z\frac{\partial w}{\partial x}\\ v(x,y,z)&=v_0(x,y,t)-z\frac{\partial w}{\partial y}\\ w(x,y,z)&=w(x,y,t)\end{aligned} \tag{2}$$

where u,v are displacement components along *x* and *y* axis, respectively, and *w* is the ultra-thin film deflection along *z* direction. In these equations,'*0*' superscript indicates displacements of a point (x,y,z) that belongs to the film mid-plane. Substitution of these equations into the linear strain-displacement relations, $2\varepsilon_{ij}=(u_{i.j}+u_{j.i})$, yields:

$$\begin{aligned}
\varepsilon_{xx}(x,y,z) &= \frac{\partial u_0}{\partial x} - z\frac{\partial^2 w}{\partial x^2} \\
\varepsilon_{yy}(x,y,z) &= \frac{\partial v_0}{\partial y} - z\frac{\partial^2 w}{\partial y^2} \\
\varepsilon_{xy}(x,y,z) &= \frac{1}{2}\left(\frac{\partial u_0}{\partial y} + \frac{\partial v_0}{\partial x} - 2z\frac{\partial^2 w}{\partial x \partial y}\right)
\end{aligned} \tag{3}$$

The equation of motion for Kirchhoff ultra-thin film can be written as[23];

$$\begin{aligned}
&\frac{\partial N_{xx}}{\partial x} + \frac{\partial N_{xy}}{\partial y} = \rho h \frac{\partial^2 u}{\partial t^2} \\
&\frac{\partial N_{yy}}{\partial y} + \frac{\partial N_{xy}}{\partial x} = \rho h \frac{\partial^2 v}{\partial t^2} \\
&\frac{\partial^2 M_{xx}}{\partial x^2} + 2\frac{\partial^2 M_{xy}}{\partial x \partial y} + \frac{\partial^2 M_{yy}}{\partial y^2} = \rho h \frac{\partial^2 w}{\partial t^2}
\end{aligned} \tag{4}$$

where h and ρ denote the ultra-thin film thickness and the mass density, respectively. N_{ij} and M_{ij} are stress resultants, which are defined as follows:

$$\begin{aligned}
N_{ji} &= \int_{-\frac{h}{2}}^{+\frac{h}{2}} t_{ji}\, dz \\
M_{ji} &= \int_{-\frac{h}{2}}^{+\frac{h}{2}} z t_{ji}\, dz
\end{aligned} \tag{5}$$

The stress resultants N_{ij} and M_{ij} can be explicitly written according to the general nonlocal theory by integrating both sides of equation (1), as follows:

$$\begin{aligned}
(1-\varepsilon_1\nabla^2)(1-\varepsilon_2\nabla^2)N_{xx} &= \lambda(1-\varepsilon_2\nabla^2)\int_{-\frac{h}{2}}^{\frac{h}{2}}\left(\varepsilon_{xx}+\varepsilon_{yy}\right)dz + 2\mu(1-\varepsilon_1\nabla^2)\int_{-\frac{h}{2}}^{\frac{h}{2}}\varepsilon_{xx}\,dz \\
(1-\varepsilon_1\nabla^2)(1-\varepsilon_2\nabla^2)N_{yy} &= \lambda(1-\varepsilon_2\nabla^2)\int_{-\frac{h}{2}}^{\frac{h}{2}}\left(\varepsilon_{xx}+\varepsilon_{yy}\right)dz + 2\mu(1-\varepsilon_1\nabla^2)\int_{-\frac{h}{2}}^{\frac{h}{2}}\varepsilon_{yy}\,dz \\
(1-\varepsilon_1\nabla^2)(1-\varepsilon_2\nabla^2)N_{xy} &= 2\mu(1-\varepsilon_1\nabla^2)\int_{-h/2}^{h/2}\varepsilon_{xy}\,dz
\end{aligned} \tag{6}$$

$$(1-\varepsilon_1\nabla^2)(1-\varepsilon_2\nabla^2)M_{xx}=\lambda(1-\varepsilon_2\nabla^2)\int_{-h/2}^{h/2} z\left(\varepsilon_{xx}+\varepsilon_{yy}\right)dz+2\mu(1-\varepsilon_1\nabla^2)\int_{-h/2}^{h/2} z\varepsilon_{xx}\,dz$$

$$(1-\varepsilon_1\nabla^2)(1-\varepsilon_2\nabla^2)M_{yy}=\lambda(1-\varepsilon_2\nabla^2)\int_{-h/2}^{h/2} z\left(\varepsilon_{xx}+\varepsilon_{yy}\right)dz+2\mu(1-\varepsilon_1\nabla^2)\int_{-h/2}^{h/2} z\varepsilon_{yy}\,dz$$

$$(1-\varepsilon_1\nabla^2)(1-\varepsilon_2\nabla^2)M_{xy}=2\mu(1-\varepsilon_1\nabla^2)\int_{-h/2}^{h/2} z\varepsilon_{xy}\,dz$$

where $\nabla^2=(\frac{\partial^2}{\partial x^2}+\frac{\partial^2}{\partial y^2})$ is 2D-Laplacian operator.

To form the balance equations in terms of the thin film displacements, equation (3) was substituted into equation (6) and the result was substituted into equation (4), which gave:

$$\lambda h(1-\varepsilon_2\nabla^2)(\frac{\partial^2 u_0}{\partial x^2}+\frac{\partial^2 v_0}{\partial x\partial y})+2\mu h(1-\varepsilon_1\nabla^2)(\frac{\partial^2 u_0}{\partial x^2})+\mu h(1-\varepsilon_1\nabla^2)(\frac{\partial^2 u_0}{\partial y^2}+\frac{\partial^2 v_0}{\partial x\partial y})$$
$$-\rho h\frac{\partial^2 u_0}{\partial t^2}[1-(\varepsilon_1+\varepsilon_2)\nabla^2+\varepsilon_1\varepsilon_2\nabla^4]=0$$

$$\lambda h(1-\varepsilon_2\nabla^2)(\frac{\partial^2 u_0}{\partial x\partial y}+\frac{\partial^2 v_0}{\partial y^2})+2\mu h(1-\varepsilon_1\nabla^2)(\frac{\partial^2 v_0}{\partial y^2})+\mu h(1-\varepsilon_1\nabla^2)(\frac{\partial^2 u_0}{\partial x\partial y}+\frac{\partial^2 v_0}{\partial x^2})$$
$$-\rho h\frac{\partial^2 v_0}{\partial t^2}[1-(\varepsilon_1+\varepsilon_2)\nabla^2+\varepsilon_1\varepsilon_2\nabla^4]=0 \qquad (7)$$

$$\frac{\lambda h^3}{12}(1-\varepsilon_2\nabla^2)(\frac{\partial^4 w}{\partial x^4}+\frac{\partial^4 w}{\partial y^4}+2\frac{\partial^4 w}{\partial y^2\partial x^2})+\frac{\mu h^3}{6}(1-\varepsilon_1\nabla^2)(\frac{\partial^4 w}{\partial x^4}+\frac{\partial^4 w}{\partial y^4}+2\frac{\partial^4 w}{\partial y^2\partial x^2})$$
$$+\rho h\frac{\partial^2 w}{\partial t^2}[1-(\varepsilon_1+\varepsilon_2)\nabla^2+\varepsilon_1\varepsilon_2\nabla^4]=0$$

3. Free vibration of ultra-thin film

To express the derived equations of motion for the free vibration regime of the ultra-thin film, the displacement field is considered as:

$$u(x,y,t)=U(x,y)e^{i\omega t}$$
$$v(x,y,t)=V(x,y)e^{i\omega t} \qquad (8)$$
$$w(x,y,t)=W(x,y)e^{i\omega t}$$

where ω is natural frequency, and $U(x,y)$, $V(x,y)$, and $W(x,y)$ are shape functions. The substitution of equation (8) into equation (7) gives:

$$\lambda h(1-\varepsilon_2\nabla^2)(\frac{\partial^2 U}{\partial x^2}+\frac{\partial^2 V}{\partial x\partial y})+2\mu h(1-\varepsilon_1\nabla^2)(\frac{\partial^2 U}{\partial x^2})+\mu h(1-\varepsilon_1\nabla^2)(\frac{\partial^2 U}{\partial y^2}+\frac{\partial^2 V}{\partial x\partial y})$$
$$+\rho h\omega^2 U[1-(\varepsilon_1+\varepsilon_2)\nabla^2+\varepsilon_1\varepsilon_2\nabla^4]=0$$

$$\lambda h(1-\varepsilon_2\nabla^2)(\frac{\partial^2 U}{\partial x\partial y}+\frac{\partial^2 V}{\partial y^2})+2\mu h(1-\varepsilon_1\nabla^2)(\frac{\partial^2 V}{\partial y^2})+\mu h(1-\varepsilon_1\nabla^2)(\frac{\partial^2 U}{\partial x\partial y}+\frac{\partial^2 V}{\partial x^2}) \quad (9)$$
$$+\rho h\omega^2 V[1-(\varepsilon_1+\varepsilon_2)\nabla^2+\varepsilon_1\varepsilon_2\nabla^4]=0$$

$$\frac{\lambda h^3}{12}(1-\varepsilon_2\nabla^2)(\frac{\partial^4 W}{\partial x^4}+\frac{\partial^4 W}{\partial y^4}+2\frac{\partial^4 W}{\partial y^2\partial x^2})+\frac{\mu h^3}{6}(1-\varepsilon_1\nabla^2)(\frac{\partial^4 W}{\partial x^4}+\frac{\partial^4 W}{\partial y^4}+2\frac{\partial^4 W}{\partial y^2\partial x^2})$$
$$-\rho h\omega^2 W[1-(\varepsilon_1+\varepsilon_2)\nabla^2+\varepsilon_1\varepsilon_2\nabla^4]=0$$

Equation (13) can be rewritten utilizing the following non-dimensional parameters:

$$X=\frac{x}{L_x},\ Y=\frac{y}{L_y},\ R=\frac{L_x}{L_y},\ \eta_1=\frac{\varepsilon_1}{L_y^2},\ \eta_2=\frac{\varepsilon_2}{L_y^2},\ D_1=\frac{\lambda\eta_2+2\mu\eta_1}{\lambda+2\mu}$$
$$D_2=\frac{\mu\eta_1}{\lambda+2\mu},\ D_3=\frac{\lambda\eta_2+3\mu\eta_1}{\lambda+2\mu},\ D_4=\frac{\mu}{\lambda+2\mu},\ D_5=\frac{\lambda\eta_2+\mu\eta_1}{\lambda+2\mu},\ D_6=\frac{\mu+\lambda}{\lambda+2\mu} \quad (10)$$

as follows:

$$-\left(\frac{D_1}{R^2}\right)\frac{\partial^4 U}{\partial X^4}-(D_3)\frac{\partial^4 U}{\partial X^2\,\partial Y^2}-(D_2R^2)\frac{\partial^4 U}{\partial Y^4}+\frac{\partial^2 U}{\partial X^2}+(D_4R^2)\frac{\partial^2 U}{\partial Y^2}-(D_5R)\frac{\partial^4 V}{\partial X\,\partial Y^3}$$
$$-\left(\frac{D_5}{R}\right)\frac{\partial^4 V}{\partial X^3\,\partial Y}+(D_6R)\frac{\partial^2 V}{\partial X\,\partial Y}$$
$$=\Omega^2\left[U-(\frac{\eta_1+\eta_2}{R^2})\frac{\partial^2 U}{\partial X^2}-(\eta_1+\eta_2)\frac{\partial^2 U}{\partial Y^2}+(\frac{\eta_1\eta_2}{R^4})\frac{\partial^4 U}{\partial X^4}\right.$$
$$\left.+(\frac{2\eta_1\eta_2}{R^2})\frac{\partial^4 U}{\partial X^2\,\partial Y^2}+(\eta_1\eta_2)\frac{\partial^4 U}{\partial Y^4}\right]$$

$$-\left(\frac{D_2}{R^2}\right)\frac{\partial^4 V}{\partial X^4}-(D_3)\frac{\partial^4 V}{\partial X^2\,\partial Y^2}-(D_1R^2)\frac{\partial^4 V}{\partial Y^4}+(D_4)\frac{\partial^2 V}{\partial X^2}+\left(\frac{1}{R^2}\right)\frac{\partial^2 V}{\partial Y^2}-(D_5R)\frac{\partial^4 U}{\partial X\,\partial Y^3}$$
$$-\left(\frac{D_5}{R}\right)\frac{\partial^4 U}{\partial X^3\,\partial Y}+(D_6R)\frac{\partial^2 U}{\partial X\,\partial Y}$$
$$=\Omega^2\left[V-(\frac{\eta_1+\eta_2}{R^2})\frac{\partial^2 V}{\partial X^2}-(\eta_1+\eta_2)\frac{\partial^2 V}{\partial Y^2}+(\frac{\eta_1\eta_2}{R^4})\frac{\partial^4 V}{\partial X^4}\right. \quad (11)$$
$$\left.+(\frac{2\eta_1\eta_2}{R^2})\frac{\partial^4 V}{\partial X^2\,\partial Y^2}+(\eta_1\eta_2)\frac{\partial^4 V}{\partial Y^4}\right]$$

$$\left[\frac{\partial^4 W}{\partial X^4}+2R^2\frac{\partial^4 W}{\partial X^2\partial Y^2}+R^4\frac{\partial^4 W}{\partial Y^4}\right]-D_1\left[\frac{1}{R^2}\frac{\partial^6 W}{\partial X^6}+3\frac{\partial^6 W}{\partial X^4\partial Y^2}+3R^2\frac{\partial^6 W}{\partial X^2\partial Y^4}+R^4\frac{\partial^6 W}{\partial Y^6}\right]=$$

$$\Lambda^2\left[W-\left(\eta_1+\eta_2\right)\frac{1}{R^2}\frac{\partial^2 W}{\partial X^2}-\left(\eta_1+\eta_2\right)\frac{\partial^2 W}{\partial Y^2}+\frac{\eta_1\eta_2}{R^4}\frac{\partial^4 W}{\partial X^4}+\frac{2\eta_1\eta_2}{R^2}\frac{\partial^4 W}{\partial X^2\partial Y^2}+\eta_1\eta_2\frac{\partial^4 W}{\partial Y^4}\right]$$

where L_x and L_y are the film length and width, respectively. $\Omega^2 = \frac{\rho\omega^2 {L_x}^2}{\lambda+2\mu}$ is a non-dimensional frequency of the in-plane vibration, and $\Lambda^2 = \frac{12\rho\omega^2 {L_x}^4}{(\lambda+2\mu)h^2}$ is the non-dimensional frequency for the out-of-plane vibration of the thin film. Next, equations (11) are solved using the differential quadrature method (DQM). Actually, DQM employed weighting coefficients and sufficient mesh points to convert the initial and boundary value problems into a system of algebraic equations with convenient solutions. DQM has many valuable advantages over other numerical methods such as high accuracy, simplicity, and fast convergence.

3.1. Differential quadrature method (DQM)

In this section and based on DQM, the Chebyshev–Gauss–Lobatto distribution is considered to discretize the problem domain in x and y directions:

$$x_i = \frac{1}{2}\left(1 - \cos\left(\frac{i-1}{N_x - 1}\pi\right)\right) \qquad i = 1. \ldots . N_x \tag{12}$$

$$y_j = \frac{1}{2}\left(1 - \cos\left(\frac{j-1}{N_y - 1}\pi\right)\right) \qquad j = 1. \ldots . N_y \tag{13}$$

N_x and N_y are the numbers of mesh points in the elastic domain.

In the context of the DQM, weighted functions are employed to express the derivatives of a two-dimensional function, $f(x,y)$, at a mesh point (x_i, y_i) as follows[41]:

$$\left.\frac{\partial^n f(x,y)}{\partial x^n}\right|_{(x_i,y_j)} = \sum_{k=1}^{N_x} \Lambda_{ik}^{x(n)} f(x_k, y_j) \tag{14}$$

$$\left.\frac{\partial^m f(x,y)}{\partial y^m}\right|_{(x_i,y_j)} = \sum_{l=1}^{N_y} \Lambda_{jl}^{y(m)} f(x_i, y_l) \tag{15}$$

$$\left.\frac{\partial^{n+m} f(x,y)}{\partial x^n\, \partial y^m}\right|_{(x_i,y_j)} = \sum_{k=1}^{N_x}\sum_{l=1}^{N_y} \Lambda_{ik}^{x(n)} \Lambda_{jl}^{y(m)} f(x_k, y_l) \tag{16}$$

where, $i = 1,..,N_x$, $j = 1,..,N_y$ and $\Lambda_{ik}^{x(n)}$, $\Lambda_{jl}^{y(m)}$ are weighting coefficients described as the following. For n=1 and m=1, The weighting coefficients related to the 1st derivative with respect to x and y are expressed as [41]:

$$\Lambda_{ik}^{x(1)} = \begin{cases} \dfrac{\Gamma(x_i)}{(x_i - x_k)\Gamma(x_k)} & for\ i \neq k \\ -\displaystyle\sum_{\substack{k=1 \\ i\neq k}}^{N_x} \Lambda_{ik}^{x(1)} & for\ i = k \end{cases} \tag{17a}$$

$$\Lambda_{jl}^{y(1)} = \begin{cases} \dfrac{\Gamma(y_j)}{(y_j - y_l)\Gamma(y_l)} & for\ j \neq l \\ -\sum\limits_{\substack{l=1 \\ j \neq l}}^{N_y} \Lambda_{jl}^{y(1)} & for\ j = l \end{cases} \tag{17b}$$

where $\Gamma(x_i)$ is Lagrangian polynomials described as:

$$\Gamma(x_i) = \prod_{\substack{k=1 \\ i \neq k}}^{N_x} (x_i - x_k) \tag{18a}$$

$$\Gamma(y_j) = \prod_{\substack{l=1 \\ j \neq l}}^{N_y} (y_j - y_l) \tag{18b}$$

The weighting coefficients relevant to higher-order derivatives could be expressed as [41]:

$$\Lambda_{ik}^{x(n)} = \sum_{p=1}^{N_x} \Lambda_{ip}^{x(n-1)} \Lambda_{pk}^{x(1)} \tag{19a}$$

$$\Lambda_{jl}^{y(m)} = \sum_{p=1}^{N_y} \Lambda_{jp}^{y(m-1)} \Lambda_{pl}^{y(1)} \tag{19b}$$

Therefore, the resultant form of governing equations of motion after employing DQM are as the following:

$$\begin{aligned} &-\left(\frac{D_1}{R^2}\right)\sum_{k=1}^{N_x} \Lambda_{ik}^{x(4)} U_{kj} - (D_2 R^2) \sum_{l=1}^{N_y} \Lambda_{jl}^{y(4)} U_{il} - (D_3) \sum_{k=1}^{N_x}\sum_{l=1}^{N_y} \Lambda_{ik}^{x(2)} \Lambda_{jl}^{y(2)} U_{kl} \\ &\quad + \sum_{k=1}^{N_x} \Lambda_{ik}^{x(2)} U_{kj} + (D_4 R^2) \sum_{l=1}^{N_y} \Lambda_{jl}^{y(2)} U_{il} + (D_5 R) \sum_{k=1}^{N_x}\sum_{l=1}^{N_y} \Lambda_{ik}^{x(1)} \Lambda_{jl}^{y(3)} V_{kl} \\ &\quad + \left(\frac{D_5}{R}\right) \sum_{k=1}^{N_x}\sum_{l=1}^{N_y} \Lambda_{ik}^{x(3)} \Lambda_{jl}^{y(1)} V_{kl} - (D_6 R) \sum_{k=1}^{N_x}\sum_{l=1}^{N_y} \Lambda_{ik}^{x(1)} \Lambda_{jl}^{y(1)} V_{kl} \\ &\quad = \Omega^2 \left[U_{ij} - \left(\frac{\eta_1 + \eta_2}{R^2}\right) \sum_{k=1}^{N_x} \Lambda_{ik}^{x(2)} U_{kj} - (\eta_1 + \eta_2) \sum_{l=1}^{N_y} \Lambda_{jl}^{y(2)} U_{il} \right. \\ &\quad + \left(\frac{\eta_1 \eta_2}{R^4}\right) \sum_{k=1}^{N_x} \Lambda_{ik}^{x(4)} U_{kj} + \left(\frac{2\,\eta_1 \eta_2}{R^2}\right) \sum_{k=1}^{N_x}\sum_{l=1}^{N_y} \Lambda_{ik}^{x(2)} \Lambda_{jl}^{y(2)} U_{kl} \\ &\quad \left. + (\eta_1 \eta_2) \sum_{l=1}^{N_y} \Lambda_{jl}^{y(4)} U_{il} \right] \end{aligned} \tag{20-a}$$

$$
\begin{aligned}
&-\left(\frac{D_2}{R^2}\right)\sum_{l=1}^{N_y}\Lambda_{jl}^{y(4)}V_{il}-(D_1R^2)\sum_{k=1}^{N_x}\Lambda_{ik}^{x(4)}V_{kj}-(D_3)\sum_{k=1}^{N_x}\sum_{l=1}^{N_y}\Lambda_{ik}^{x(2)}\Lambda_{jl}^{y(2)}V_{kl}\\
&\quad+\left(\frac{1}{R^2}\right)\sum_{l=1}^{N_y}\Lambda_{jl}^{y(2)}V_{il}+(D_4)\sum_{k=1}^{N_x}\Lambda_{ik}^{x(2)}V_{kj}-\left(\frac{D_5}{R}\right)\sum_{k=1}^{N_x}\sum_{l=1}^{N_y}\Lambda_{ik}^{x(3)}\Lambda_{jl}^{y(1)}U_{kl}\\
&\quad-(D_5R)\sum_{k=1}^{N_x}\sum_{l=1}^{N_y}\Lambda_{ik}^{x(1)}\Lambda_{jl}^{y(3)}U_{kl}+(D_6R)\sum_{k=1}^{N_x}\sum_{l=1}^{N_y}\Lambda_{ik}^{x(1)}\Lambda_{jl}^{y(1)}U_{kl}\\
&\quad=\Omega^2\left[V_{ij}-\left(\frac{\eta_1+\eta_2}{R^2}\right)\sum_{k=1}^{N_x}\Lambda_{ik}^{x(2)}V_{kj}-(\eta_1+\eta_2)\sum_{l=1}^{N_y}\Lambda_{jl}^{y(2)}V_{il}\right.\\
&\quad+\left(\frac{\eta_1\eta_2}{R^4}\right)\sum_{k=1}^{N_x}\Lambda_{ik}^{x(4)}V_{kj}+\left(\frac{2\eta_1\eta_2}{R^2}\right)\sum_{k=1}^{N_x}\sum_{l=1}^{N_y}\Lambda_{ik}^{x(2)}\Lambda_{jl}^{y(2)}V_{kl}\\
&\quad\left.+(\eta_1\eta_2)\sum_{l=1}^{N_y}\Lambda_{jl}^{y(4)}V_{il}\right]
\end{aligned}
\tag{20-b}
$$

$$
\begin{aligned}
&\left[\sum_{k=1}^{N_x}\Lambda_{ik}^{x(4)}W_{kj}+2R^2\sum_{k=1}^{N_x}\sum_{l=1}^{N_y}\Lambda_{ik}^{x(2)}\Lambda_{jl}^{y(2)}W_{kl}+R^4\sum_{l=1}^{N_y}\Lambda_{jl}^{y(4)}W_{il}\right]\\
&\quad-D_1\left[\frac{1}{R^2}\sum_{k=1}^{N_x}\Lambda_{ik}^{x(6)}W_{kj}+3\sum_{k=1}^{N_x}\sum_{l=1}^{N_y}\Lambda_{ik}^{x(4)}\Lambda_{jl}^{y(2)}W_{kl}\right.\\
&\quad\left.+3R^2\sum_{k=1}^{N_x}\sum_{l=1}^{N_y}\Lambda_{ik}^{x(2)}\Lambda_{jl}^{y(4)}W_{kl}+R^4\sum_{l=1}^{N_y}\Lambda_{jl}^{y(6)}W_{il}\right]\\
&\quad=\Lambda^2\left[W_{ij}-\left(\eta_1+\eta_2\right)\frac{1}{R^2}\sum_{k=1}^{N_x}\Lambda_{ik}^{x(2)}W_{kj}-\left(\eta_1+\eta_2\right)\sum_{l=1}^{N_y}\Lambda_{jl}^{y(2)}W_{il}\right.\\
&\quad+\frac{\eta_1\eta_2}{R^4}\sum_{k=1}^{N_x}\Lambda_{ik}^{x(4)}W_{kj}+\frac{2\eta_1\eta_2}{R^2}\sum_{k=1}^{N_x}\sum_{l=1}^{N_y}\Lambda_{ik}^{x(2)}\Lambda_{jl}^{y(2)}W_{kl}\\
&\quad\left.+\eta_1\eta_2\sum_{l=1}^{N_y}\Lambda_{jl}^{y(4)}W_{il}\right]
\end{aligned}
\tag{20-c}
$$

where $V_{ij}=V(x_i,y_j)$, $U_{ij}=U(x_i,y_j)$ and $W_{ij}=W(x_i,y_j)$.

Equations (20-a) and (20-b) can be represented as:

$$[K^*]\{Z\} = \Omega^2[M^*]\{Z\} \tag{21}$$

In which

$$\{Z\} = \begin{Bmatrix} U \\ V \end{Bmatrix} \tag{22}$$

$\left[K^*\right]$ and $\left[M^*\right]$ are stiffness and mass matrices established with correct arrangement of the elements from equations (20-a), (20-b) and introduced as:

$$\left[K^*\right] = \begin{bmatrix} \mathbf{K}_{uu} & \mathbf{K}_{uv} \\ \mathbf{K}_{vu} & \mathbf{K}_{vv} \end{bmatrix} \tag{23}$$

$$\left[M^*\right] = \begin{bmatrix} \mathbf{M}_{uu} & \mathbf{0} \\ \mathbf{0} & \mathbf{M}_{vv} \end{bmatrix} \tag{24}$$

(24)

To eigenvalue analysis, equation (21) and BCs should be satisfied simultaneously. Consequently, applying boundary conditions to equation (21) and separating the boundary and domain mesh points lead to:

$$\begin{bmatrix} \mathbf{K}_{bb} & \mathbf{K}_{bd} \\ \mathbf{K}_{db} & \mathbf{K}_{dd} \end{bmatrix} \begin{Bmatrix} \{Z_b\} \\ \{Z_d\} \end{Bmatrix} - \Omega^2 \begin{bmatrix} \mathbf{0} & \mathbf{0} \\ \mathbf{M}_{db} & \mathbf{M}_{dd} \end{bmatrix} \begin{Bmatrix} \{Z_b\} \\ \{Z_d\} \end{Bmatrix} = 0 \tag{25}$$

Where the subscriptions b and d show boundary and domain mesh points, respectively. Hence,

$$\mathbf{K}_{bb}\{Z_b\} + \mathbf{K}_{bd}\{Z_d\} = 0 \tag{26}$$

$$\mathbf{K}_{db}\{Z_b\} + \mathbf{K}_{dd}\{Z_d\} - \Omega^2\left(\mathbf{M}_{db}Z_b + \mathbf{M}_{dd}\{Z_d\}\right) = 0 \tag{27}$$

Rewriting Equation (26):

$$\{Z_b\} = -\mathbf{K}_{bb}^{-1}\mathbf{K}_{bd}\{Z_d\} \tag{28}$$

Substituting Eq. (28) into Eq. (27) leads to:

$$\left(\mathbf{K}_{dd} - \mathbf{K}_{db}\mathbf{K}_{bb}^{-1}\mathbf{K}_{bd}\right)\{Z_d\} - \Omega^2\left(\mathbf{M}_{dd} - \mathbf{M}_{db}\mathbf{K}_{bb}^{-1}\mathbf{K}_{bd}\right)\{Z\} = 0 \tag{29}$$

In compact form, Eq. (29) is rewritten as:

$$[\bar{K}^*]\{Z_d\} = \Omega^2[\bar{M}^*]\{Z_d\} \tag{30}$$

In which:

$$[\bar{K}^*] = \mathbf{K}_{dd} - \mathbf{K}_{db}\,\mathbf{K}_{bb}^{-1}\mathbf{K}_{bd} \tag{31}$$

$$[\bar{M}^*] = \mathbf{M}_{dd} - \mathbf{M}_{db}\mathbf{K}_{bb}^{-1}\mathbf{K}_{bd} \tag{32}$$

Similarly, the equation governing the out-of-plane frequencies can be derived from Eq. (20-c) as the following:

$$\begin{bmatrix} \tilde{K}_{dd} & \tilde{K}_{db} \\ \tilde{K}_{bd} & \tilde{K}_{bb} \end{bmatrix}\begin{bmatrix} W_d \\ W_b \end{bmatrix} = \Lambda^2 \begin{bmatrix} \tilde{M}_{dd} & \tilde{M}_{db} \\ \tilde{M}_{bd} & \tilde{M}_{bb} \end{bmatrix}\begin{bmatrix} W_d \\ W_b \end{bmatrix} \tag{33}$$

where, $\tilde{K}_{ii}$ and $\tilde{M}_{ii}$ $(i = b,d)$ are the elements of the stiffness and mass matrices obtained by properly arranging the elements from Eq. (20-c). Similar to in-plane vibration, separating the boundary and domain mesh points lead to:

$$[\bar{K}]\{W_d\} = \Lambda^2[\bar{M}]\{W_d\} \tag{34}$$

In which:

$$[\bar{K}] = \tilde{K}_{dd} - \tilde{K}_{db}\tilde{K}_{bb}^{-1}\tilde{K}_{bd} \tag{35}$$

$$[\bar{M}] = \tilde{M}_{dd} - \tilde{M}_{db}\tilde{M}_{bb}^{-1}\tilde{M}_{bd} \tag{35}$$

The in-plane non-dimensional frequency Ω and its corresponding normalized mode shape can be obtained by solving the eigenvalue problem (Eq. (30)). On the other hand, the out-of-plane non-dimensional frequency Λ and its corresponding normalized mode shape can be obtained by solving the eigenvalue problem (Eq. (34)).

4. Results and discussion

4.1. Free in-plane vibrations

Numerical results are extracted to show the merit of the general nonlocal theory over Eringen's nonlocal theory. To this end, the natural frequencies of the in-plane and flexural vibrations of Simply-Supported (SSSS) ultra-thin film are determined.

Since the purpose of the current study is the parametric analysis, the constant nonlocal parameters ε_1 and ε_2 are considered from negative to positive values [18], although the negative value of the coefficients may be physically meaningless.

We present in Figure 1 the nonlocal effect on the in-plane natural frequencies of ultra-thin film with Aspect Ratio = 1 (i.e., $L_x = L_y$). The results of the general nonlocal model are compared to the ones obtained based on Eringen's nonlocal model. Indeed, the general nonlocal model outweighs Eringen's nonlocal model in accounting for the difference between the longitudinal and transverse nonlocal fields of the material. Thus, we present the frequency ratio (i.e. $\frac{\text{Nonlocal frequency}}{\text{local frequency}}$) (Figs. 1(a) and (b)) and the non-dimensional frequency (i.e., Ω) (Figs. 1(c) and (d)) for different values of the non-dimensional nonlocal parameters $\eta_1 = (\varepsilon_1 / L_y^2)$ and $\eta_2 = (\varepsilon_2 / L_y^2)$. It follows from Fig. 1 that the general nonlocal model is sensitive to the difference between normal and shear nonlocal fields where different frequencies are obtained when tailoring $\frac{\eta_1}{\eta_2}$ ratio from -2 to 2.

Eringen's nonlocal model reflects a softening effect of the nonlocal field on film mechanics. As shown in Fig. 1, the in-plane natural frequency decreases below one of the local models where a frequency ratio lower than one was obtained. However, the general nonlocal model reflects all possible effects of nonlocal fields on the film mechanics. The natural frequency will increase if one of the two nonlocal parameters is negative (Fig. 1). For example, the frequency ratio > 1 for $\frac{\eta_1}{\eta_2}$ a film with =-2 with either η_1 or η_2 is negative (Figs. 1(a) and 1(b)). The frequency is further increased when both η_1 and η_2 are of negative values.

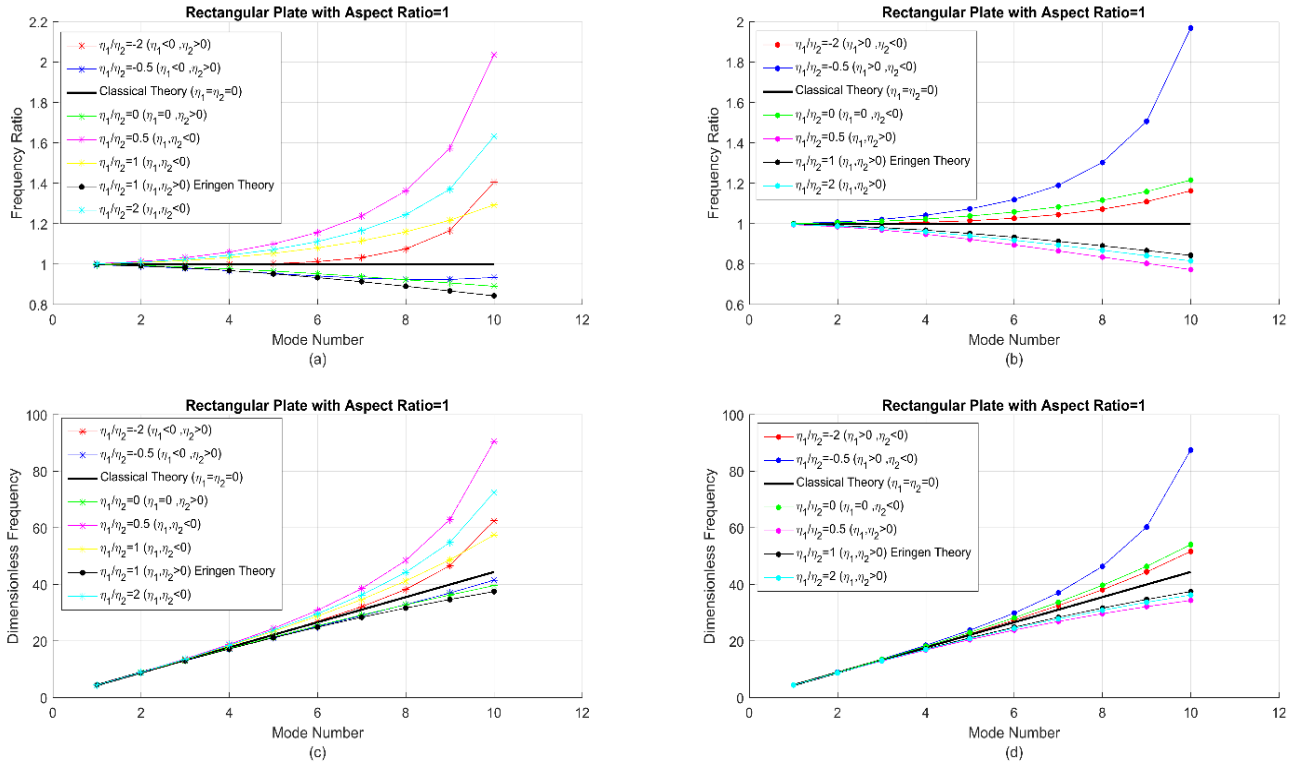

Fig. 1: Comparison of Eringen's and classical theories with General nonlocal theory for Free in-plane vibration of nano ultra-thin film based on the sign of η_1, η_2 ($\eta_1 = cte$)

(a) frequency ratio (b) frequency ratio (c) Dimensionless frequency (d) Dimensionless frequency

The effects of aspect ratio on free in-plane vibration are considered in figure (2) to figure (5). In the figures, the variation of frequency ratio is presented for different dimensionless ratio (η_1/η_2) and 1st, 2nd, 5th, and 10th modes separately. The results are reported based on the different values of the dimensionless ratio of $\frac{\eta_1}{\eta_2}$ from -5 to 5 in four different states.

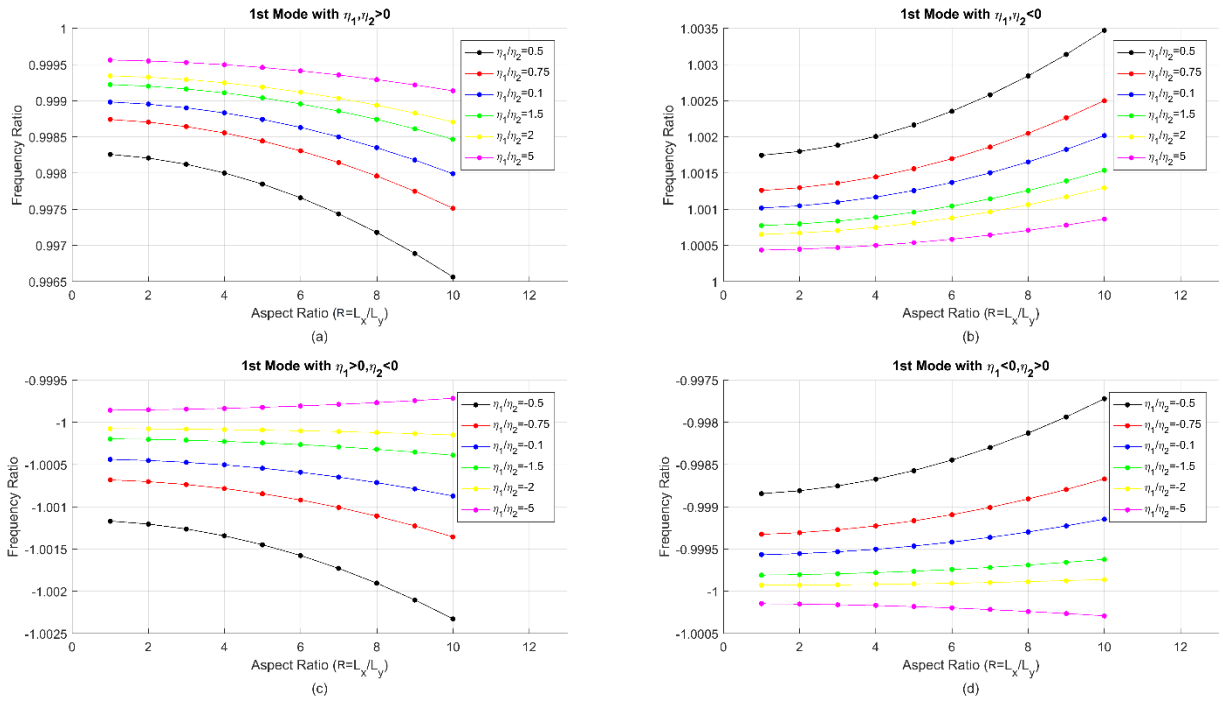

Fig. 2: Variation of frequency ratio for free in-plane vibration by changing aspect ratio for 1st Mode.

a) $\eta_1, \eta_2 > 0$ b) $\eta_1, \eta_2 < 0$ c) $\eta_1 > 0, \eta_2 < 0$ d) $\eta_1 < 0, \eta_2 > 0$

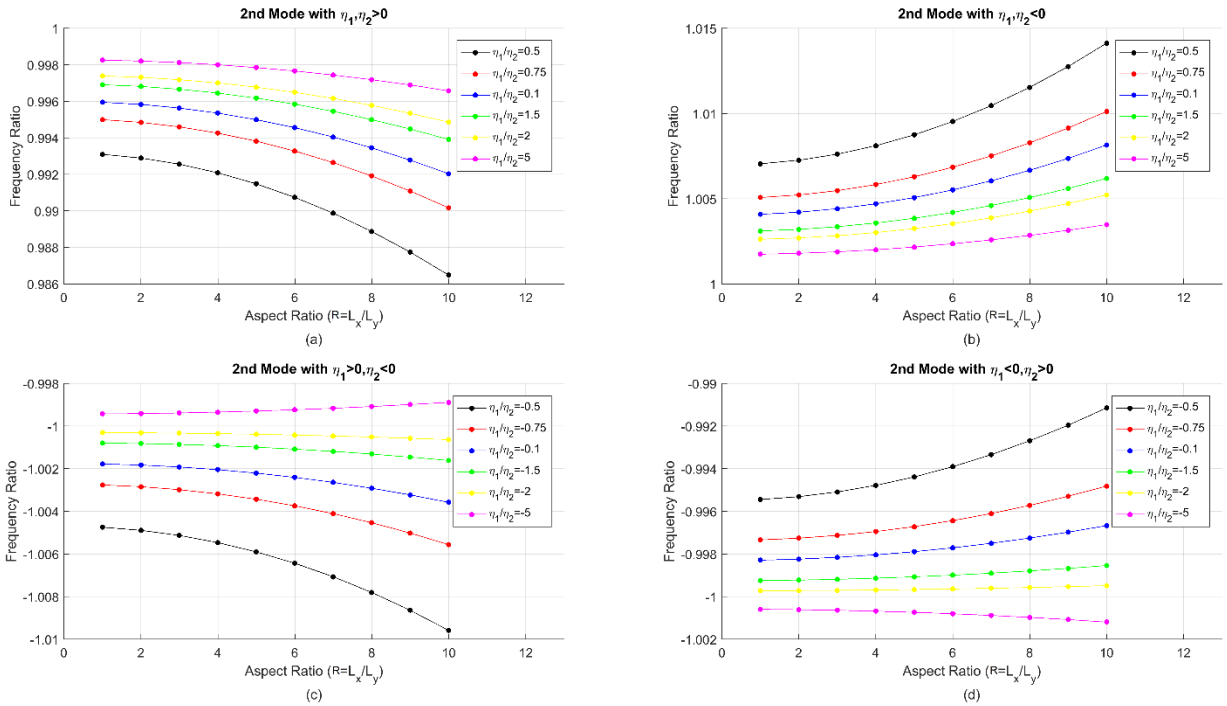

Fig. 3: Variation of frequency ratio for free in-plane vibration by changing aspect ratio for 2nd Mode.

a) $\eta_1, \eta_2 > 0$ b) $\eta_1, \eta_2 < 0$ c) $\eta_1 > 0, \eta_2 < 0$ d) $\eta_1 < 0, \eta_2 > 0$

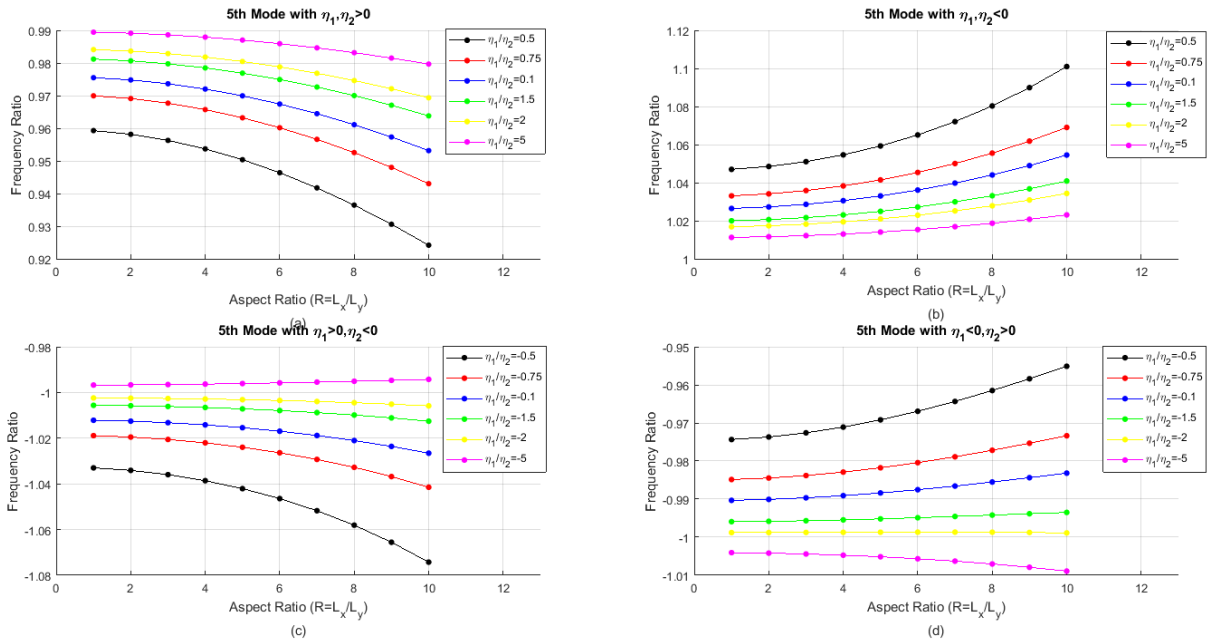

Fig. 4: Variation of frequency ratio for free in plane vibration by changing aspect ratio for 5th Mode.

a) $\eta_1, \eta_2 > 0$ b) $\eta_1, \eta_2 < 0$ c) $\eta_1 > 0, \eta_2 < 0$ d) $\eta_1 < 0, \eta_2 > 0$

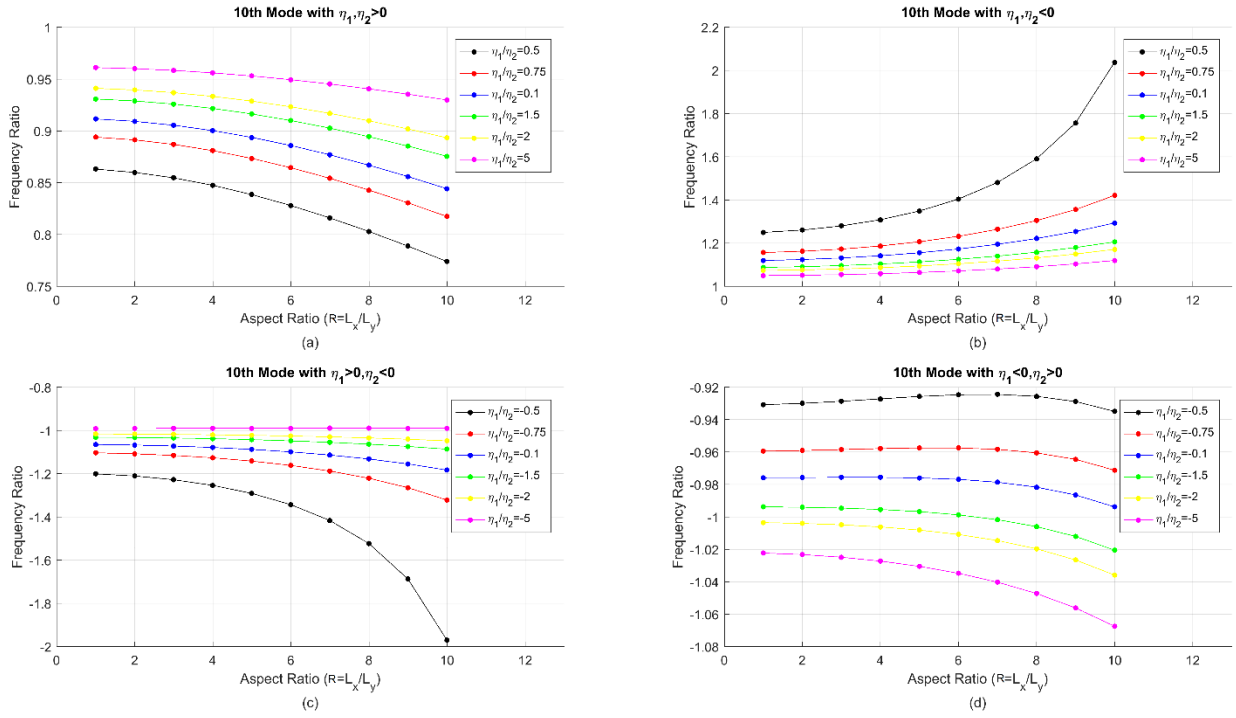

Fig. 5: Variation of frequency ratio for free in plane vibration by changing aspect ratio for 10th Mode.

a) $\eta_1, \eta_2 > 0$ b) $\eta_1, \eta_2 < 0$ c) $\eta_1 > 0, \eta_2 < 0$ d) $\eta_1 < 0, \eta_2 > 0$

As it is observed, in figures(2-a),(3-a),(4-a),(5-a), where both η_1 and η_2 are positive, the frequency ratio decreases with increasing the aspect ratio. Also, in figures (2-b), (3-b), (4-b), (5-b), the frequency ratio increases with increasing the aspect ratio when both η_1 and η_2 are of negative values. Either η_1 or η_2 is negative; the frequency ratio indicates antithetical behavior based on the mode number and the different values of $\frac{\eta_1}{\eta_2}$.

Variation of frequency ratio vs. the length of x-direction for nano ultra-thin film in aspect ratio 1 are illustrated in figure(6) to figure(9) for 1st, 2nd, 5th, and 10th modes, respectively.

The results are illustrated based on the different values of the dimensionless ratio of $\frac{\eta_1}{\eta_2}$ from -5 to 5 in four different states according to the sign of η_1, η_2.

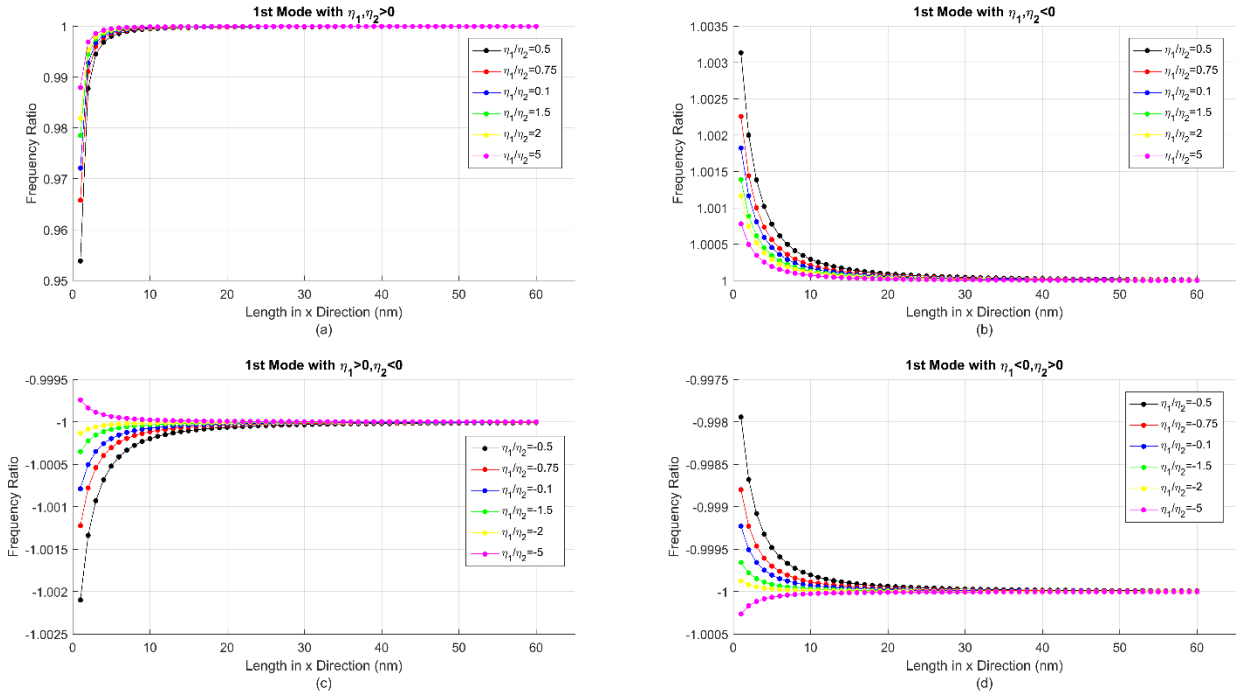

Fig. 6: variation of frequency ratio with length of nano ultra-thin film for different nonlocal parameters ratio for 1st Mode, with

a) $\eta_1, \eta_2 > 0$ b) $\eta_1, \eta_2 < 0$ c) $\eta_1 > 0, \eta_2 < 0$ d) $\eta_1 < 0, \eta_2 > 0$

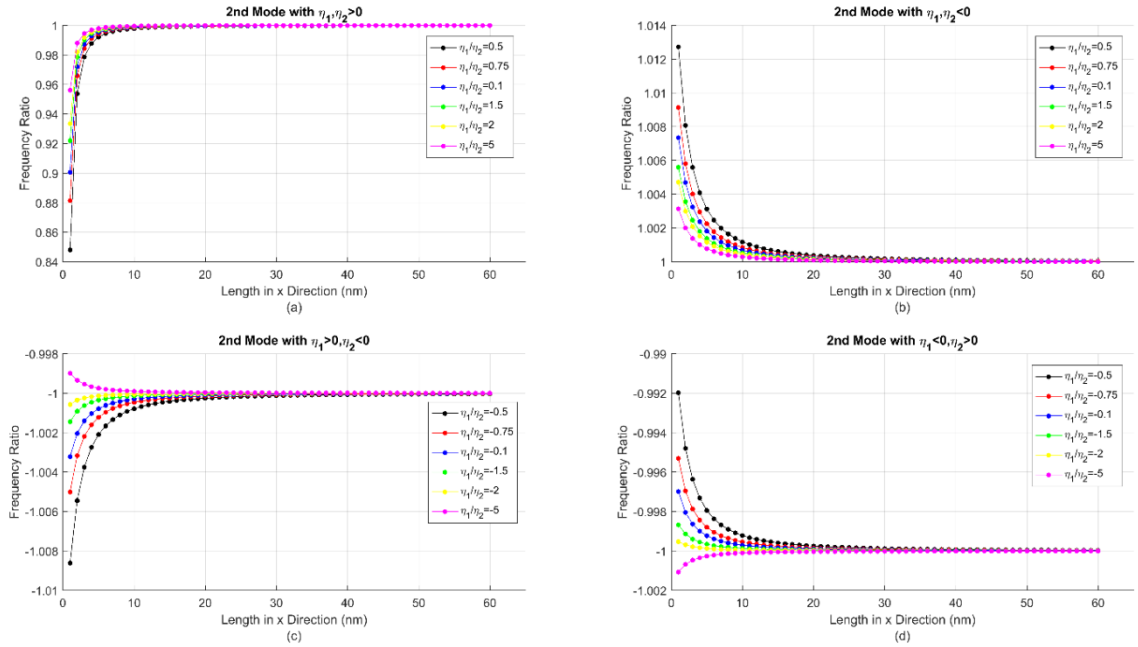

Fig. 7: variation of frequency ratio with length of nano ultra-thin film for different nonlocal parameters ratio for 2nd Mode, with

a) $\eta_1, \eta_2 > 0$ b) $\eta_1, \eta_2 < 0$ c) $\eta_1 > 0, \eta_2 < 0$ d) $\eta_1 < 0, \eta_2 > 0$

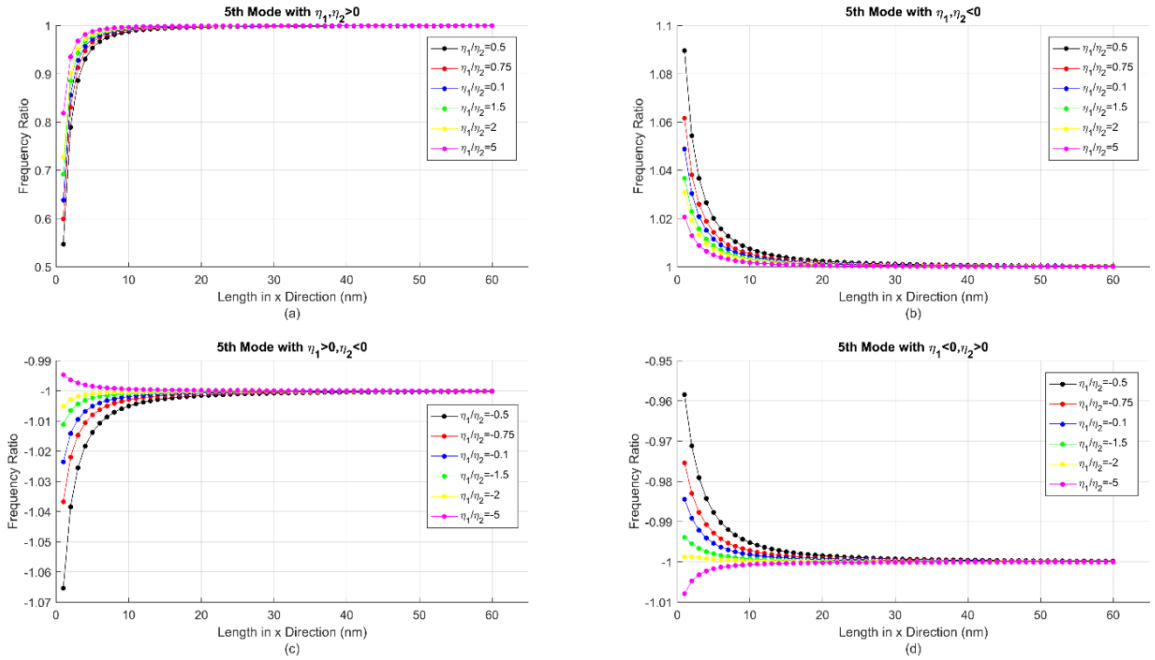

Fig. 8: variation of frequency ratio with length of nano ultra-thin film for different nonlocal parameters ratio for 5th Mode, with

a) $\eta_1, \eta_2 > 0$ b) $\eta_1, \eta_2 < 0$ c) $\eta_1 > 0, \eta_2 < 0$ d) $\eta_1 < 0, \eta_2 > 0$

Figures (6) to (9) illustrate that for all different modes number and different values of $\frac{\eta_1}{\eta_2}$, the frequency ratio achieves the constant value of 1 or -1 by increasing L_x .

In Table (1), the frequency ratios are illustrated for free in-plane vibration of nano ultra-thin film for different boundary condition. The results are obtained for the 1^{st} , 3^{rd} , 5^{th} and 10^{th} in-plane vibration modes with aspect ratio 1 and different values of $\frac{\eta_1}{\eta_2}$.

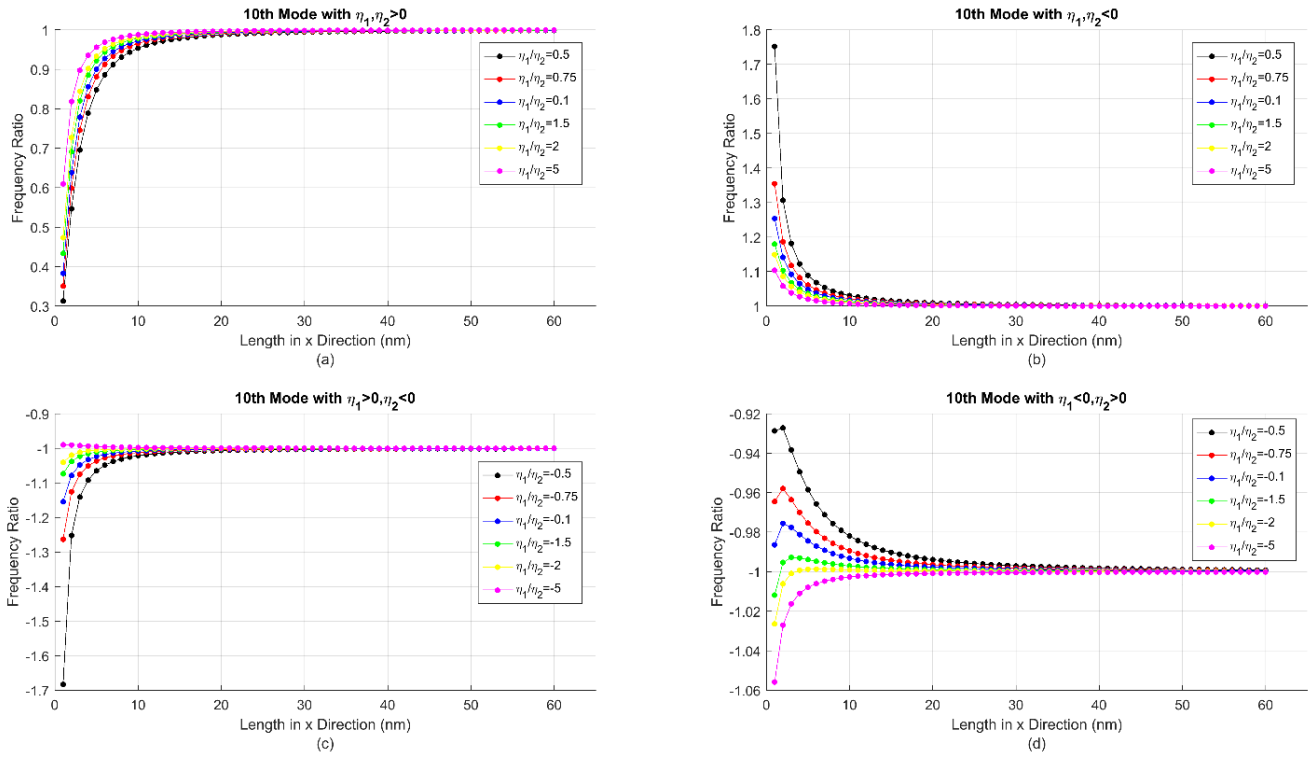

Fig. 9: variation of frequency ratio with length of nano ultra-thin film for different nonlocal parameters ratio for 10^{th} Mode, with

$$a)\ \eta_1,\eta_2>0 \quad b)\ \eta_1,\eta_2<0 \quad c)\ \eta_1>0,\eta_2<0 \quad d)\ \eta_1<0,\eta_2>0$$

4.2. Free out of plane vibrations

In this section, the free out of plane vibrations of the Kirchhoff ultra-thin film are reported based on the general nonlocal theory and compared to the Eringen's and Local theories.

Figure (10) displays the effects of nonlocal parameters η_1 and η_2 $(\eta_1,\eta_1>0)$ on the frequency ratio of ultra-thin film for different values of aspect ratio. For all values of aspect ratio, the results have descending trend with increasing mode number. It is obvious, the gradient of

frequency ratio gets smoother with increasing aspect ratio. Also, with increasing the value of $\frac{\eta_1}{\eta_2}$, the frequency ratio increases.

Table 1. variation of frequency ratio for different nonlocal parameters and different boundary condition for free in-plane vibrations

		$\eta_1 = 0.022$, and η_2 changes by variation of the (η_1 / η_2)				
B.C	mode	0.5	0.75	1	1.5	2
CCCC	*1st*	0.95029	0.96102	0.96844	0.97796	0.98371
	3st	0.71639	0.72286	0.72677	0.73132	0.73391
	5st	0.55693	0.56532	0.57017	0.57575	0.57899
	10st	0.49015	0.49774	0.50210	0.50898	0.50968
SCCS	*1st*	0.88958	0.89416	0.89729	0.90127	0.90371
	3st	0.69649	0.70035	0.70265	0.70531	0.70681
	5st	0.55043	0.55708	0.56082	0.56497	0.56725
	10st	0.48199	0.49031	0.49487	0.49974	0.50229
SSCS	*1st*	0.88412	0.88781	0.89038	0.89377	0.89591
	3st	0.69170	0.69382	0.69491	0.69592	0.69634
	5st	0.54829	0.55349	0.55634	0.55941	0.56104
	10st	0.47890	0.48739	0.49193	0.49669	0.49916
SCCC	*1st*	0.89767	0.90431	0.90903	0.91537	0.91945
	3st	0.70193	0.70770	0.71125	0.71541	0.71778
	5st	0.55251	0.56057	0.56512	0.57018	0.57295
	10st	0.48690	0.49458	0.49891	0.50359	0.50609

The effects of aspect ratio on free out of plane vibration are considered in figure (11). In the figure, the variation of frequency ratio is presented for different dimensionless ratio (η_1 / η_2) and 1st, 2nd, 5th and 10th modes separately. The results are reported based on the different values of the dimensionless ratio of $\frac{\eta_1}{\eta_2}$ from 0.5 to 10. For all values of $\frac{\eta_1}{\eta_2}$ and mode numbers, the frequency ratio achieves a constant value but with different slop. For high values of $\frac{\eta_1}{\eta_2}$ and

lower modes, the frequency ratio gets faster to the constant value. Also, as it is mentioned before, with increasing the value of $\frac{\eta_1}{\eta_2}$, the frequency ratio increases.

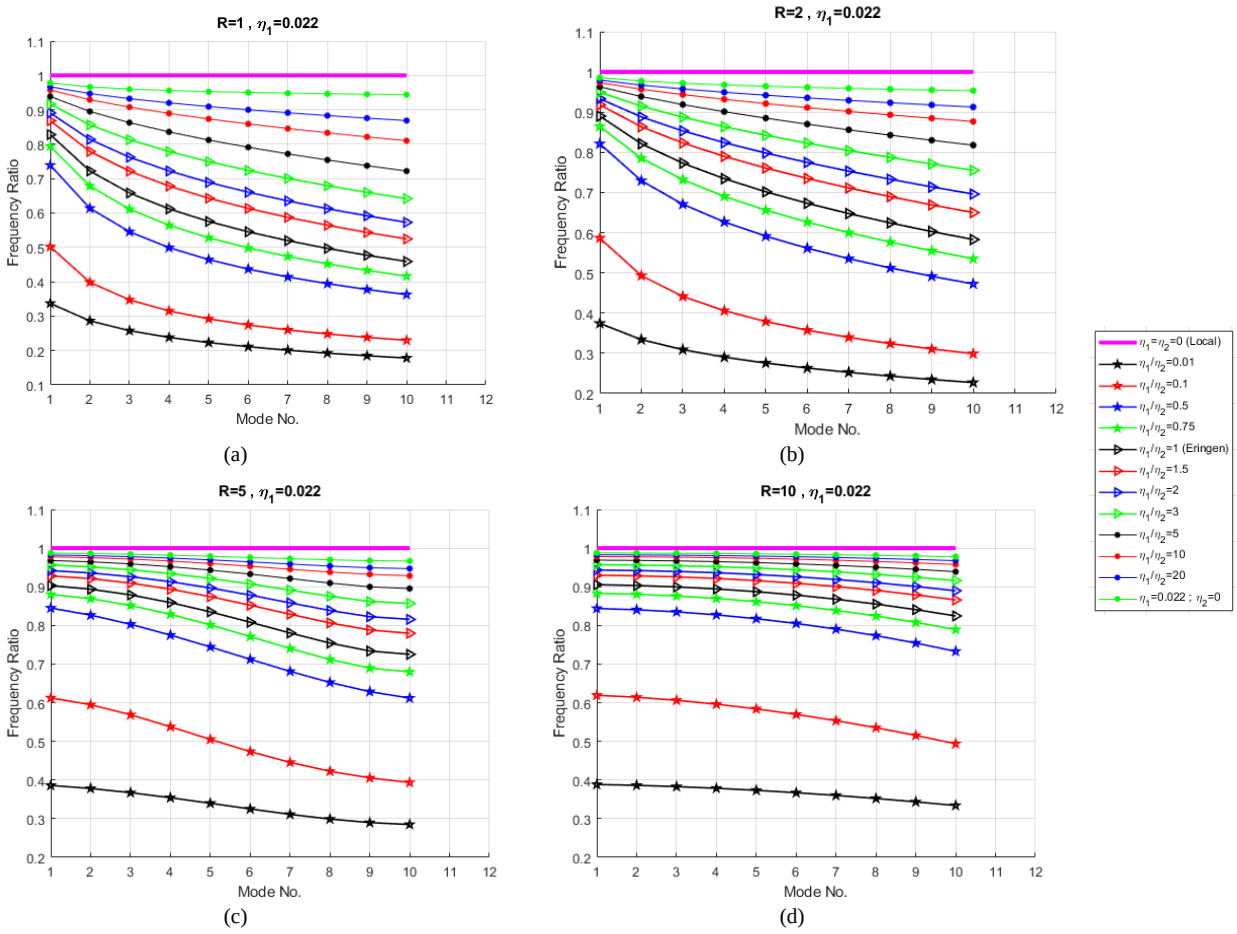

Fig. 10: Comparison of Eringen's and Local theories with General nonlocal theory for Free out of plane vibration of nano ultra-thin film based on the different value of $\frac{\eta_1}{\eta_2}$: (a) Aspect Ratio=1 (b) Aspect Ratio=2 (c) Aspect Ratio=5 (d) Aspect Ratio=10

The effects of boundary conditions on the out of plane natural frequencies of ultra-thin film with aspect ratio=2 are reported in figures (11) and (12) based on local theory and 3 different values of $\frac{\eta_1}{\eta_2} = 0.5, 1, 2$. In figure (11), the non-dimensional frequencies for the first ten modes are displaced according to six different types of boundary conditions. As it is clear, the highest and lowest frequencies are relevant to CCCC and SSSS boundary conditions. Hence, non-

dimensional frequencies for mentioned local and nonlocal states are plotted in figure (12) for CCCC and SSSS boundary conditions.

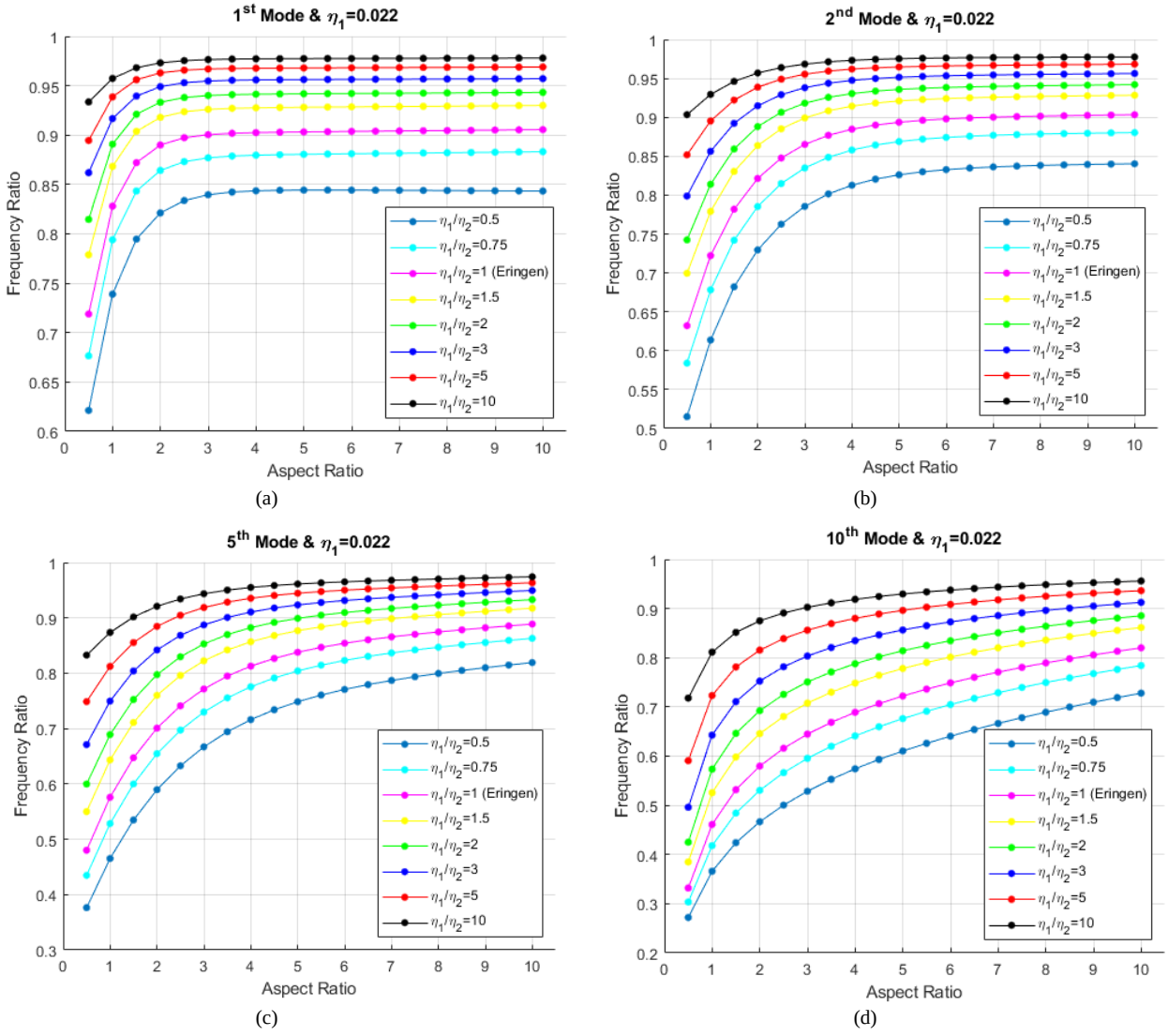

Fig. 10: Variation of frequency ratio for out of plane vibration by changing aspect ratio

1st Mode b) 2nd Mode c) 5th Mode d) 10th Mode

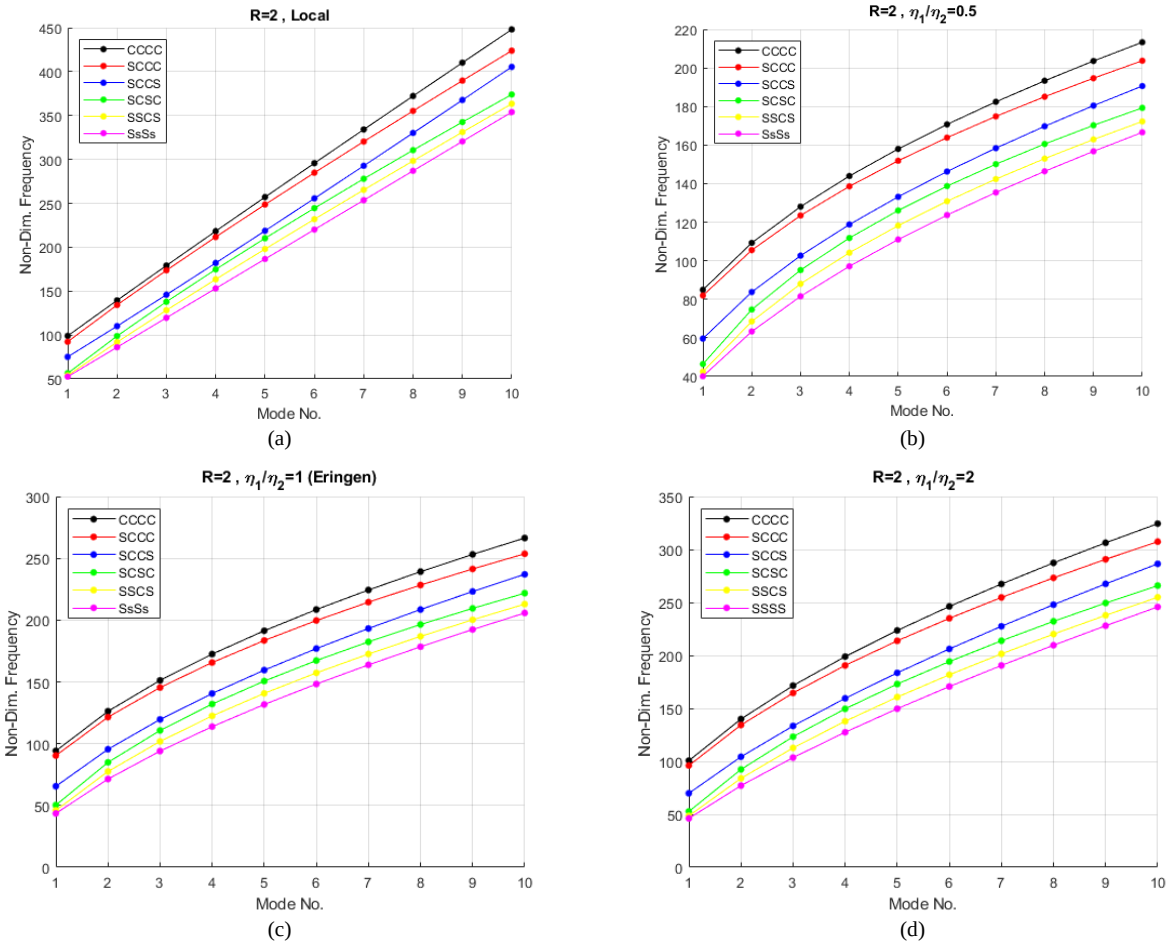

Fig. 11: Variation of frequency ratio for out of plane vibration by changing aspect ratio

Local b) $\eta_1/\eta_2=0.5$ c) Eringen d) $\eta_1/\eta_2=2$

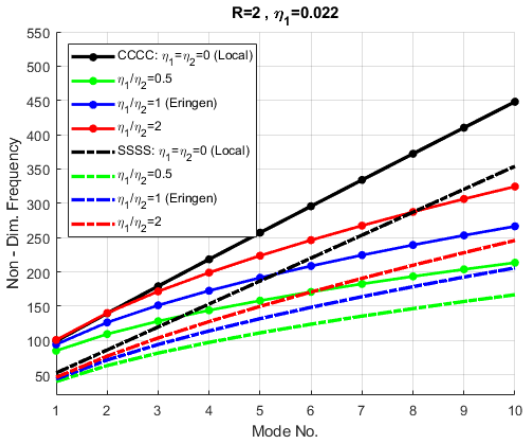

Fig. 12: Non-Dimensional frequency for SSSS and CCCC nano-plate (Aspect Ration=2)

5. Conclusion

The goal of this paper is to investigate the in-plane and the out of plane free vibrational behavior of the Kirchhoff nano ultra-thin film. To do so, the general nonlocal model is employed to establish the mathematical model of the ultra-thin film. Also, DQM is applied to obtain the results and calculate the frequencies. Since the in-plane and out of plane vibration of the nano ultra-thin film is independent of each other, the analysis is considered independently. In addition, the effects of two constant nonlocal parameters, aspect ratios and length in x-direction on the dimensionless frequencies and frequency ratio, are presented and discussed in detail. Also, the effects of different boundary conditions are considered. As it is concluded, the general nonlocal model is sensitive to the difference between normal and shear nonlocal fields where different frequencies are obtained.

References

[1] R.A. Toupin, Theories of elasticity with couple-stress, 17 (1964) 85-112.
[2] R.D. Mindlin, H.F. Tiersten, Effects of couple-stresses in linear elasticity, in, COLUMBIA UNIV NEW YORK, 1962, pp. 415-448.
[3] W. Kolter, Couple stresses in the theory of elasticity, Proc. Koninklijke Nederl. Akaad. van Wetensch, 67 (1964) 20.
[4] N.A. Fleck, J.W. Hutchinson, A phenomenological theory for strain gradient effects in plasticity, Journal of the Mechanics and Physics of Solids, 41 (1993) 1825-1857.
[5] E.C. Aifantis, Gradient deformation models at nano, micro, and macro scales, (1999).
[6] A.C. Eringen, On differential equations of nonlocal elasticity and solutions of screw dislocation and surface waves, Journal of applied physics, 54 (1983) 4703-4710.
[7] A.C. Eringen, Nonlocal polar elastic continua, International journal of engineering science, 10 (1972) 1-16.
[8] A.C. Eringen, Theory of micropolar plates, Zeitschrift für angewandte Mathematik und Physik ZAMP, 18 (1967) 12-30.
[9] A.M. Zenkour, M. Sobhy, A simplified shear and normal deformations nonlocal theory for bending of nanobeams in thermal environment, Physica E: Low-Dimensional Systems and Nanostructures, 70 (2015) 121-128.
[10] J.W. Yan, L.H. Tong, C. Li, Y. Zhu, Z.W. Wang, Exact solutions of bending deflections for nano-beams and nano-plates based on nonlocal elasticity theory, Composite Structures, 125 (2015) 304-313.
[11] F. Ebrahimi, M.R. Barati, Buckling analysis of nonlocal strain gradient axially functionally graded nanobeams resting on variable elastic medium, Proceedings of the Institution of Mechanical Engineers, Part C: Journal of Mechanical Engineering Science, 232 (2018) 2067-2078.
[12] H. Daghigh, V. Daghigh, A. Milani, D. Tannant, T.E. Lacy Jr, J.N. Reddy, Nonlocal bending and buckling of agglomerated CNT-reinforced composite nanoplates, Composites Part B: Engineering, 183 (2020) 107716.
[13] O. Rahmani, O. Pedram, Analysis and modeling the size effect on vibration of functionally graded nanobeams based on nonlocal Timoshenko beam theory, International Journal of Engineering Science, 77 (2014) 55-70.
[14] F. Ebrahimi, M.R. Barati, Vibration analysis of size-dependent flexoelectric nanoplates incorporating surface and thermal effects, Mechanics of Advanced Materials and Structures, 25 (2018) 611-621.
[15] F. Ebrahimi, M.R. Barati, P. Haghi, Wave propagation analysis of size-dependent rotating inhomogeneous nanobeams based on nonlocal elasticity theory, Journal of Vibration and Control, 24 (2018) 3809-3818.
[16] B. Karami, D. Shahsavari, M. Janghorban, Wave propagation analysis in functionally graded (FG) nanoplates under in-plane magnetic field based on nonlocal strain gradient theory and four variable refined plate theory, Mechanics of Advanced Materials and Structures, 25 (2018) 1047-1057.
[17] R. Sourki, S.A. Hosseini, Coupling effects of nonlocal and modified couple stress theories incorporating surface energy on analytical transverse vibration of a weakened nanobeam, The European Physical Journal Plus, 132 (2017) 1-14.
[18] H.B. Khaniki, Vibration analysis of rotating nanobeam systems using Eringen's two-phase local/nonlocal model, Physica E: Low-dimensional Systems and Nanostructures, 99 (2018) 310-319.
[19] H. Arvin, The flapwise bending free vibration analysis of micro-rotating Timoshenko beams using the differential transform method, Journal of Vibration and Control, 24 (2018) 4868-4884.

[20] R. Ansari, V. Mohammadi, M.F. Shojaei, R. Gholami, S. Sahmani, On the forced vibration analysis of Timoshenko nanobeams based on the surface stress elasticity theory, Composites Part B: Engineering, 60 (2014) 158-166.
[21] H.B. Khaniki, On vibrations of FG nanobeams, International Journal of Engineering Science, 135 (2019) 23-36.
[22] S. Bhattacharya, D. Das, Free vibration analysis of bidirectional-functionally graded and double-tapered rotating micro-beam in thermal environment using modified couple stress theory, Composite Structures, 215 (2019) 471-492.
[23] S.C. Pradhan, T. Murmu, Application of nonlocal elasticity and DQM in the flapwise bending vibration of a rotating nanocantilever, Physica E: Low-Dimensional Systems and Nanostructures, 42 (2010) 1944-1949.
[24] J. Fang, D. Zhou, Y. Dong, Three-dimensional vibration of rotating functionally graded beams, Journal of Vibration and Control, 24 (2018) 3292-3306.
[25] J. Fang, J. Gu, H. Wang, Size-dependent three-dimensional free vibration of rotating functionally graded microbeams based on a modified couple stress theory, International Journal of Mechanical Sciences, 136 (2018) 188-199.
[26] R. Talebitooti, S.O. Rezazadeh, A. Amiri, Comprehensive semi-analytical vibration analysis of rotating tapered AFG nanobeams based on nonlocal elasticity theory considering various boundary conditions via differential transformation method, Composites Part B: Engineering, 160 (2019) 412-435.
[27] S.S. Mirjavadi, B. Mohasel Afshari, N. Shafiei, S. Rabby, M. Kazemi, Effect of temperature and porosity on the vibration behavior of two-dimensional functionally graded micro-scale Timoshenko beam, Journal of Vibration and Control, 24 (2018) 4211-4225.
[28] C.M.C. Roque, P. Martins, A.J.M. Ferreira, R.M.N. Jorge, Differential evolution for free vibration optimization of functionally graded nano beams, Composite Structures, 156 (2016) 29-34.
[29] N. Shafiei, S.S. Mirjavadi, B. MohaselAfshari, S. Rabby, M. Kazemi, Vibration of two-dimensional imperfect functionally graded (2D-FG) porous nano-/micro-beams, Computer Methods in Applied Mechanics and Engineering, 322 (2017) 615-632.
[30] A.R. Shahidi, A. Anjomshoa, S.H. Shahidi, M. Kamrani, Fundamental size dependent natural frequencies of non-uniform orthotropic nano scaled plates using nonlocal variational principle and finite element method, Applied Mathematical Modelling, 37 (2013) 7047-7061.
[31] M. Arefi, M.H. Zamani, M. Kiani, Size-dependent free vibration analysis of three-layered exponentially graded nanoplate with piezomagnetic face-sheets resting on Pasternak's foundation, Journal of Intelligent Material Systems and Structures, 29 (2018) 774-786.
[32] F. Ebrahimi, M.R. Barati, Damping vibration analysis of smart piezoelectric polymeric nanoplates on viscoelastic substrate based on nonlocal strain gradient theory, Smart Materials and Structures, 26 (2017) 065018.
[33] B. Karami, D. Shahsavari, M. Janghorban, L. Li, Free vibration analysis of FG nanoplate with poriferous imperfection in hygrothermal environment, Structural Engineering and Mechanics, 73 (2020) 191-207.
[34] H.u. Liu, Q. Zhang, X. Yang, J. Ma, Size-dependent vibration of laminated composite nanoplate with piezo-magnetic face sheets, Engineering with Computers, (2021) 1-17.
[35] A.A. Daikh, A. Drai, I. Bensaid, M.S.A. Houari, A. Tounsi, On vibration of functionally graded sandwich nanoplates in the thermal environment, Journal of Sandwich Structures & Materials, (2020) 1099636220909790.
[36] S. Faroughi, S.M.H. Goushegir, Free in-plane vibration of heterogeneous nanoplates using Ritz method, Journal of Theoretical and Applied Vibration and Acoustics, 2 (2016) 1-20.
[37] Z. Rahimi, W. Sumelka, S.R. Ahmadi, D. Baleanu, Study and control of thermoelastic damping of in-plane vibration of the functionally graded nano-plate, Journal of Vibration and Control, 25 (2019) 2850-2862.
[38] M. Shaat, A. Abdelkefi, New insights on the applicability of Eringen's nonlocal theory, International Journal of Mechanical Sciences, 121 (2017) 67-75.
[39] S. Faroughi, A. Rahmani, M.I. Friswell, On wave propagation in two-dimensional functionally graded porous rotating nano-beams using a general nonlocal higher-order beam model, Applied Mathematical Modelling, 80 (2020) 169-190.
[40] A. Rahmani, S. Faroughi, M.I. Friswell, The vibration of two-dimensional imperfect functionally graded (2D-FG) porous rotating nanobeams based on general nonlocal theory, Mechanical Systems and Signal Processing, 144 (2020) 106854.
[41] X. Wang, Differential quadrature and differential quadrature based element methods: theory and applications, Butterworth-Heinemann, 2015.